











Structural characterization and bioactivity profiling of the fungal peptaibiotic tolypin reveal protective effects against influenza viruses

Johanna Eichberg^{1,2}  | Markus Oberpaul^{1,2}  | Christoph Hartwig¹  |
 Andrea Helga Geißler³  | Carsten Culmsee⁴  | Andreas Vilcinskas^{1,3,5}  |
 Eva Böttcher-Friebertshäuser⁶  | Hans Brückner⁷  | Thomas Degenkolb³  |
 Kornelia Harges^{1,2,5} 

¹Branch for Bioresources of the Fraunhofer IME, Fraunhofer Institute for Molecular Biology and Applied Ecology IME, Giessen, Germany

²BMBF Junior Research Group in Infection Research "ASCRIBE", Giessen, Germany

³Department of Insect Biotechnology, Justus-Liebig-University of Giessen, Giessen, Germany

⁴Institute for Pharmacology and Clinical Pharmacy, Biochemical-Pharmacological Center Marburg, University of Marburg, Marburg, Germany

⁵LOEWE Centre for Translational Biodiversity Genomics (LOEWE-TBG), Frankfurt, Germany

⁶Institute of Virology, University of Marburg, Marburg, Germany

⁷Department of Food Sciences, Interdisciplinary Research Centre for Biosystems, Land Use and Nutrition, Justus-Liebig-University of Giessen, Giessen, Germany

Correspondence

Kornelia Harges, Branch for Bioresources of the Fraunhofer IME, Fraunhofer Institute for Molecular Biology and Applied Ecology IME, Ohlebergsweg 12, 35392 Giessen, Germany.
 Email: Kornelia.Harges@ime.fraunhofer.de

Funding information

Bundesministerium für Bildung und Forschung; German Federal Ministry for Education and Research (BMBF) under the ASCRIBE program, Grant/Award Number: 01KI2024

Abstract

In a bioprospection for new antivirals, we tested nonribosomally biosynthesized polypeptide antibiotics in MDCK II cells for their actions on influenza A and B viruses (IAV/IBV). Only tolypin, a mixture of closely related 16-residue peptaibiotics from the fungus *Tolypocladium inflatum* IE 1897, showed promising activity. It was selected for further investigation and structural characterization by ultrahigh performance liquid chromatography coupled to high-resolution mass spectrometry (UHPLC-HR-MS/MS) and ultrahigh performance liquid chromatography coupled to in-source collision-induced dissociation tandem mass spectrometry (UHPLC-isCID-HR-MS/MS), revealing 12 partially co-eluting individual peptides that were fully sequenced. Since tolypin-related efrapeptins are potent inhibitors of F₁/F_o-ATPase, we screened tolypin for its toxicity against MDCK II cells and larvae of the greater wax moth *Galleria mellonella*. We found that a nontoxic concentration of tolypin (1 µg/mL) reduced the titer of two IBV strains by 4–5 log values, and that of an H3N2 strain by 1–2 log values, but the H1N1pdm strain was not affected. The higher concentrations of tolypin were

Abbreviations: 2-DG, 2-deoxyglucose; AA, antimycin A; Aib, α-aminoisobutyric acid; ATP, adenosine triphosphate; CID, collision-induced dissociation; CPE, cytopathic effect; DMSO, dimethyl sulfoxide; ECAR, extracellular acidification rate; EFR, efrapeptin; FCCP, carbonylcyanide-*p*-trifluoromethoxyphenylhydrazone; IAV, influenza A virus; IBV, influenza B virus; isCID, in-source collision-induced dissociation; Iva, L-isovaline; MDCK II, Madin-Darby canine kidney cells II; MOI, multiplicity of infection; Nle, norleucine; NRPS, nonribosomal peptide synthetase; NRPs, nonribosomal peptides; OCR, oxygen consumption rate; OPA, *o*-phthalaldehyde; OXPHOS, oxidative phosphorylation; PIHPPE, (S)-2-amino-1-(1,5-diazabicyclo[4.3.0]non-5-ene-5-ylidene)-4-methylpentane; Pip, L-pipecolic acid; Rot, rotenone; UHPLC-HR-MS/MS, ultrahigh performance liquid chromatography coupled to high-resolution mass spectrometry; βAla, β-alanine.

This is an open access article under the terms of the [Creative Commons Attribution-NonCommercial-NoDerivs](https://creativecommons.org/licenses/by-nc-nd/4.0/) License, which permits use and distribution in any medium, provided the original work is properly cited, the use is non-commercial and no modifications or adaptations are made.

© 2024 The Author(s). *Archiv der Pharmazie* published by Wiley-VCH GmbH on behalf of Deutsche Pharmazeutische Gesellschaft.

cytostatic to MDCK II cells, shifted their metabolism from oxidative phosphorylation to glycolysis, and induced paralysis in *G. mellonella*, supporting the inhibition of F_1/F_0 -ATPase as the mode of action. Our results lay the foundations for future work to investigate the interplay between viral replication and cellular energy metabolism, as well as the development of drugs that target host factors.

KEYWORDS

cellular energy metabolism, influenza virus, microheterogeneity, *Tolypocladium*, UHPLC-HR-MS/MS

1 | INTRODUCTION

Influenza A (IAV) and B (IBV) viruses cause severe contagious infections and pose a major risk to human health. Annual influenza epidemics result in up to 5 million severe infections and 300,000–650,000 deaths.^[1] Vaccination is the most effective strategy to prevent influenza but only two drug classes have been approved worldwide for the treatment of patients and they have limited efficacy due to the rapid evolution of resistance. Further options for the treatment or prevention of acute infections are urgently needed. In particular, the identification of compounds targeting host factors instead of viral enzymes could reduce the risk of emerging resistance.

Bioresources derived from bacteria and fungi often include nonribosomal peptides (NRPs) with antiviral properties.^[2] NRPs are synthesized directly without ribosomes or messenger RNA and are rich in nonproteinogenic amino acids such as α -aminoisobutyric acid (Aib) because the nonribosomal peptide synthetase (NRPS) enzyme is more versatile than the ribosome complex (for remarks on the origin of nonribosomal building blocks see Supporting Information). NRPs often possess antimicrobial activity and are therefore known as peptide antibiotics, peptaibols, or peptaibiotics.^[3] Peptaibols such as peptaivirins, trichokonins, and trichorzins show potent activity against plant viruses such as tobacco mosaic virus (TMV) and cucumber mosaic virus (CMV).^[4–6] Trichokonins are 20-residue peptaibols from *Trichoderma pseudokoningii* SMF2 that induce local and systemic defense responses in tobacco (*Nicotiana tabacum* cv. Samsun) against TMV infection, increasing the production of pathogenesis-related reactive oxygen species and phenolic compounds, the activity of pathogenesis-related enzymes, and the expression of plant defense genes.^[4–6] The antiviral effect of trichokonins thus appears to target the host defense systems rather than viruses.

Treatment with peptaibiotics such as alamethicin F-50, trichotoxin A-40, and paracelsin induces the formation of voltage-gated ion channels in lipid bilayers, leading to antibacterial and hemolytic effects.^[7–13] Similarly, the antiprotozoal and anthelmintic properties of antiameobin involve the formation of ion channels in membranes.^[14–16] Pore formation in membranes was also observed for melittin, a 26-amino acid ribosomally synthesized peptide found in the venom of the European honey bee (*Apis mellifera*), which induces various effects on lipid bilayer membranes, including vesicle deformation, artificial pore

formation, disruption, and ultimately lysis.^[17] Besides its antimicrobial and hemolytic activity, melittin acts against non- and enveloped viruses in vitro, most probably due to virus surface interaction.^[18]

Tolypin is a mixture of NRPs originally isolated from species of the fungal genus *Tolypocladium*. The tolypin-related peptaibiotic efrageptin is a potent inhibitor of the F_1 catalytic domain of the mitochondrial F_1F_0 adenosine triphosphate (ATP) synthase (Supporting Information S1: Figure S1).^[19] This membrane-bound complex comprises a globular F_1 catalytic domain and a membrane-bound F_0 proton-translocating domain connected by central and peripheral stalks. It couples the transmembrane proton-motive force to the synthesis of ATP from ADP and P. Approximately 90% of ATP is generated in this manner.^[20] Inhibition of glycolysis and oxidative phosphorylation (OXPHOS) pathway suppressed the replication of the IAV subtype SC35M, providing another potential antiviral strategy.^[21] Following structural characterization, tolypins C–G were found to be identical to efrageptins C–G from the soil-borne *Tolypocladium* strains *Tolypocladium inflatum* IMI 202309, *T. inflatum* ARSEF #616 (= ATCC 18981 = CCF 962), and *Tolypocladium geodes* ARSEF #2684. These linear, cationic peptaibiotics contain several nonproteinogenic amino acids, including a high proportion of Aib and L-isovaline, as well as N-terminal acetyl-L-pipecolic acid (AcPip) and the unusual, amide-bound C-terminal residue (S)-2-amino-1-(1,5-diazabicyclo[4.3.0]non-5-ene-5-yl)ium-4-methylpentane (PIHPPE).^[20] The intraspecific and interspecific diversity of efrageptins has been studied in 44 strains of nine *Tolypocladium* species.^[22] The amino acid composition of the tolypin batch we used in the current study (see Table 3 further below) has been reported previously after derivatization with *o*-phthaldialdehyde (OPA)-1-thio- β -D-glucose, leucine enantiomers (D/L-Leu, D/L-Ile, D/L-*allo*-Ile, D/L-Nle) could be separated on a C_{18} high-performance liquid chromatography (HPLC) column. Using this approach, the L-amino acids Gly, Ala, β Ala (one residue each), Leu (two residues), and Aib (several residues) were detected, whereas Ile and *allo*-Ile were not.^[23] However, D/L-Iva and D/L-Pip were not included in this analysis. Pip and Iva in tolypin hydrolysates were also assigned the L-configuration in a more recent study.^[20]

The inhibitory effects of tolypin include potent insecticidal, antifungal, and antiviral properties. Organic extracts and fractions of *Tolypocladium* spp. have broad insecticidal properties, killing larvae and adults in the orders Lepidoptera, Diptera, Hemiptera, Coleoptera, and Blattodea. Inhibition has been reported against mitochondrial fractions of

Metarhizium anisopliae and *Tolypocladium niveum*.^[24] For taxonomic considerations - *Tolypocladium inflatum* vs. *Tolypocladium niveum* - see Supporting Information. Efrapeptins D, F, and G have also been applied to BHK-21 cells infected with Newcastle disease virus (NDV) and vesicular stomatitis virus (VSV), resulting in the suppression of syncytium formation and a reduced cytopathic effect (CPE) caused by blocking the expression of viral glycoproteins on the cell surface.^[25] Here we describe the detailed characterization of tolypin to determine its activity against influenza viruses. For the first time, we determined the structural heterogeneity of the tolypin peptides by UHPLC-HR-MS/MS and ultrahigh performance liquid chromatography coupled to in-source collision-induced dissociation tandem mass spectrometry (UHPLC-isCID-HR-MS/MS). Many electron transport chain inhibitors are highly toxic, so we first assessed the toxicity of tolypin in mammalian cells and in larvae of the greater wax moth (*Galleria mellonella*). We also measured the oxygen consumption rate (OCR) and extracellular acidification rate (ECAR) in mammalian cells using a Seahorse XF flowmeter. Finally, we directly measured the antiviral effects of tolypin using a subset of IAV and IBV strains. A detailed understanding of the antiviral properties of tolypin will yield insights into the dependence of viruses on host energy metabolism and could facilitate the development of new antiviral drugs that increase our preparedness for future pandemics.

2 | RESULTS AND DISCUSSION

2.1 | Cytotoxic and antiviral effects of peptaibiotics

We screened for the cytotoxic effects of alamethicin F-50, anti-amoebin, paracelsin, trichotoxin A-40, and tolypin by measuring the viability of MDCK II cells after exposure to the peptaibiotics for 48 h, compared with ionomycin as a positive control and dimethyl sulfoxide (DMSO) as a vehicle treatment (negative control). All five peptaibiotics

were tolerated by the MDCK II cells at concentrations of 1 and 10 ng/ μ L, whereas the highest concentration (100 ng/ μ L) was highly cytotoxic, except for trichotoxin A-40 (Figure 1a). The toxicity at high concentrations was unsurprising, given the pore-forming ability of the peptaibiotics and the impact on cell homeostasis. For example, the cytotoxicity of alamethicin in tobacco cells was shown to reflect membrane permeabilization^[26] and that of trichotoxin A-40 in rat mast cells was shown to involve membrane lysis.^[27]

Next, we assessed the impact of the five peptaibiotics on the replication of four influenza virus strains by measuring the virus-induced CPE in MDCK II cells. We infected the cells with A/Hamburg/05/2009 (H1N1pdm), A/Hessen/1/2003 (H3N2), B/Malaysia/2506/2004 (Malaysia/B), or B/Massachusetts/71 (Massachusetts/B) and determined the cell viability 48 h later. We used the natural broad-range serine protease inhibitor aprotinin as a control (Figure 1b).^[28] Alamethicin F-50 showed no antiviral activity against H1N1pdm, H3N2 or Malaysia/B, and only low activity against Massachusetts/B (2.6% protection). Antiamoebin showed marginal activity against H1N1pdm (0.8% protection), low activity against H3N2 (3.0% protection), and slightly higher activity against the IBV strains (11.6% and 8.0% protection against Malaysia/B and Massachusetts/B, respectively). Paracelsin showed no protective effect against IAV but low activity against IBV (5.4% and 4.7% protection against Malaysia/B and Massachusetts/B, respectively). Interestingly, trichotoxin A-40 showed moderate activity against Malaysia/B (37.8% protection) but no protection against IAV or Massachusetts/B. Tolypin treatment at 1 ng/ μ L conferred strong protection against Malaysia/B (56.9%) and Massachusetts/B (69.1%) but showed low activity against H3N2 (14.7% protection) and none against H1N1pdm. Because tolypin treatment resulted in the strongest antiviral effects, at least against IBV, we investigated the chemical and biological properties of tolypin in more detail.

The structures of the peptaibiotics exhibit characteristic microheterogeneity (Supporting Information S1: Tables S1 and S2). For example, the 16-residue anti-amoebins and tolypins are the shortest peptides used in this study. However, tolypin is the only peptide mixture containing the

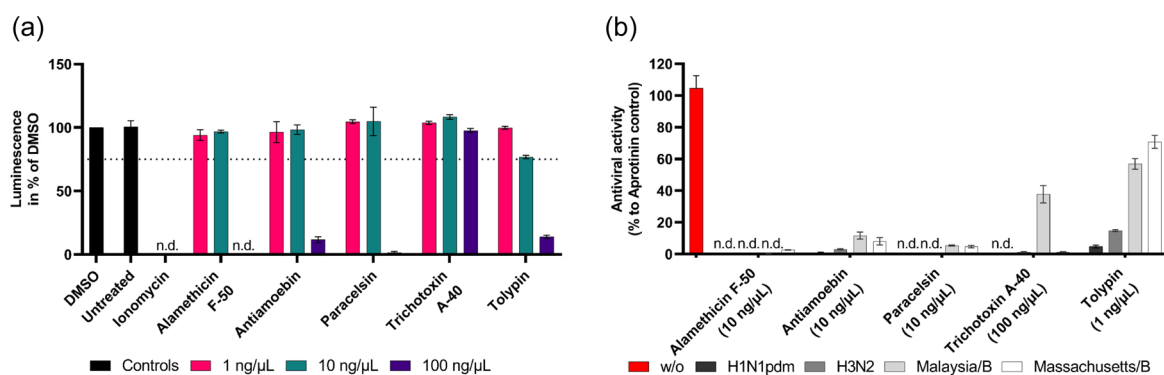


FIGURE 1 Effects of peptaibiotics on cell viability and antiviral activity. (a) MDCK II cell viability following exposure to peptaibiotics for 48 h. Cell viability was assessed by measuring adenosine triphosphate (ATP) levels using the CellTiter-Glo assay. Cell viability was normalized to the dimethyl sulfoxide (DMSO) control, which was set to 100%. The dotted line represents the cut-off value of 25% cytotoxicity in MDCK II cells. (b) Screening against influenza viruses in MDCK II cells. The cells were infected (multiplicity of infection [MOI] = 1 for H1N1pdm, H3N2, and Malaysia/B, MOI = 0.01 for Massachusetts/B) for 1 h before treatment with nontoxic concentrations of peptaibiotics, aprotinin (651 ng/ μ L) or left uninfected and untreated (w/o). After 48 h, the CellTiter-Glo Assay was used to determine cell viability. Raw luminescence values were baseline-corrected to the virus control (0%) and normalized to the aprotinin-positive control (100%). Data are means \pm SD of $n = 3$ independent measurements (n.d., not detectable).

C-terminal PHIPPE residue with its delocalized positive charge. The crystal structure suggests that efrapeptin/tolypin C interacts with F₁-ATPases mainly via hydrophobic residues.^[19] The flexibility around the βAla-Gly bond may allow the peptide domains to fit into the pocket of the enzyme for optimal hydrophobic interactions. Additionally, the crystal structure reveals numerous interactions between efrapeptin/tolypin C and ATP synthase, contributing to the binding and inhibition. For example, PHIPPE forms a polar interaction with Tyr358 (Supporting Information S1: Figure S1). Longer peptides may not fit into the binding cleft. Therefore, the length, C-terminal residue, and hydrophobicity of the peptides may play key roles in the mode of action.

2.2 | Structural analysis of tolypin

Tolypin is a mixture of linear cationic peptides with 16 residues and is dominated by tolypin F, which represents 40% of the total.^[20] For nonribosomal biosynthesis of tolypin/efrapeptin see Supporting Information. These peptides feature a labile bond between an α,α-dialkylamino acid (Aib, D-Iva, or L-Iva) and a heterocyclic secondary amino acid (Pro, Hyp, MePro, or Pip), which is preferentially cleaved during fast atom bombardment mass spectrometry (MS)^[29] and positive electrospray ionization (*ESI)-MS.^[11] This generates an N-terminal decapeptide originating from the *b*₁₀ ion, and the corresponding C-terminal hexapeptide Pip¹¹-PIHPPE¹⁶. Analysis of the tolypin mixture by UHPLC-HR-MS/MS and UHPLC-iCID-HR-MS/MS revealed the presence of at least 12 individual peptides (Table 1 and Figure 2), five of which were identical to

the corresponding efrapeptins based on low-resolution HPLC-CID-MSⁿ and chiral gas chromatography coupled to mass spectrometry (GC/MS) experiments.^[20,30] The remaining seven tolypins (C1, C2, G1, H, H2, K, and K1) were found to be minor positional isomers and homologs of the known efrapeptin/tolypin peptaibiotics (Table 1). Tolypins K and K1 are the first two efrapeptin-type sequences with the molecular formula C₈₅H₁₄₇N₁₈O₁₆.

A general building scheme can be established in which the N-terminal tripeptide AcPip¹-Aib²-Pip³ and the internal tripeptide Leu⁶-βAla⁷-Gly⁸ as well as individual residues Aib¹⁰, Pip¹¹, and Leu¹⁴ are highly conserved, whereas other positions allow exchanges with structurally related amino acids (Table 2).

All 16-residue efrapeptin-type and structurally related peptaibiotics discovered thus far feature an N-terminal AcPip residue, although we cannot exclude the possibility that acetylated 3-MePro or 4-MePro residues may be present at the N-terminus of minor compounds. Alternatively, one of the internal Pip residues could be replaced with an isobaric MePro residue. Furthermore, 16-residue sequences with an N-terminal AcPro group should not be excluded from further considerations (for further information see structural considerations in the Supporting Information). Consequently, the analysis of uncommon building blocks and isobaric amino acids requires sophisticated LC, liquid chromatography coupled to mass spectrometry, and chiral GC/MS methods for the correct assignment of the structure and stereochemistry of peptaibiotic constituents. We have demonstrated the analytical potential of UHPLC-iCID-HR-MS/MS for the sequencing and structural analysis of partially co-eluting fungal peptides.

TABLE 1 Sequences and relative quantities of individual tolypin peptides.

		y type fragment ions															(%)
		Y ₁₅	Y ₁₄	Y ₁₃	Y ₁₂	Y ₁₁	Y ₁₀	Y ₉	Y ₈	Y ₇	Y ₆	Y ₅	Y ₄	Y ₃	Y ₂	Y ₁	
C2*	Ac Pip Aib Pip Aib Ala Leu βAla Gly Aib Aib Pip Aib Ala Leu Aib PIHPPE																<1
C1*	Ac Pip Aib Pip Aib Ala Leu βAla Gly Aib Aib Pip Aib Gly Leu Iva PIHPPE																
C	Ac Pip Aib Pip Aib Aib Leu βAla Gly Aib Aib Pip Aib Gly Leu Aib PIHPPE																2
D	Ac Pip Aib Pip Aib Aib Leu βAla Gly Aib Aib Pip Aib Gly Leu Iva PIHPPE																21
E	Ac Pip Aib Pip Iva Aib Leu βAla Gly Aib Aib Pip Aib Gly Leu Iva PIHPPE																4
F	Ac Pip Aib Pip Aib Aib Leu βAla Gly Aib Aib Pip Aib Ala Leu Iva PIHPPE																40
G	Ac Pip Aib Pip Iva Aib Leu βAla Gly Aib Aib Pip Aib Ala Leu Iva PIHPPE																23
G1*	Ac Pip Aib Pip Aib Aib Leu βAla Gly Aib Aib Pip Iva Ala Leu Iva PIHPPE																2
H*	Ac Pip Aib Pip Iva Aib Leu βAla Gly Iva Aib Pip Aib Ala Leu Iva PIHPPE																5
H2*	Ac Pip Aib Pip Iva Aib Leu βAla Gly Aib Aib Pip Iva Ala Leu Iva PIHPPE																2
K1*	Ac Pip Aib Pip Iva Iva Leu βAla Gly Aib Aib Pip Iva Ala Leu Iva PIHPPE																<1
K*	Ac Pip Aib Pip Iva Iva Leu βAla Gly Iva Aib Pip Aib Ala Leu Iva PIHPPE																<1
		<i>b</i> ₁	<i>b</i> ₂	<i>b</i> ₃	<i>b</i> ₄	<i>b</i> ₅	<i>b</i> ₆	<i>b</i> ₇	<i>b</i> ₈	<i>b</i> ₉	<i>b</i>₁₀	<i>b</i> ₁₁	<i>b</i> ₁₂	<i>b</i> ₁₃	<i>b</i> ₁₄	<i>b</i> ₁₅	<i>b</i> ₁₆
		b type fragment ions															

Note: New sequences are marked with an asterisk (*). Amino acid exchange positions are highlighted in bold. Relative abundancies are shown as percentages. The diagnostic N-terminal and C-terminal fragment ions are shown in Supporting Information S1: Table S3. The diagnostic fragment ions resulting from the *y*₆ ions are shown in Supporting Information S1: Table S4. Sum formulae, calculated ion masses, and mass deviations from Supporting Information S1: Tables S1 and S2 can be found in Supporting Information S1: Tables S5–S11. *y*-type fragment ions.

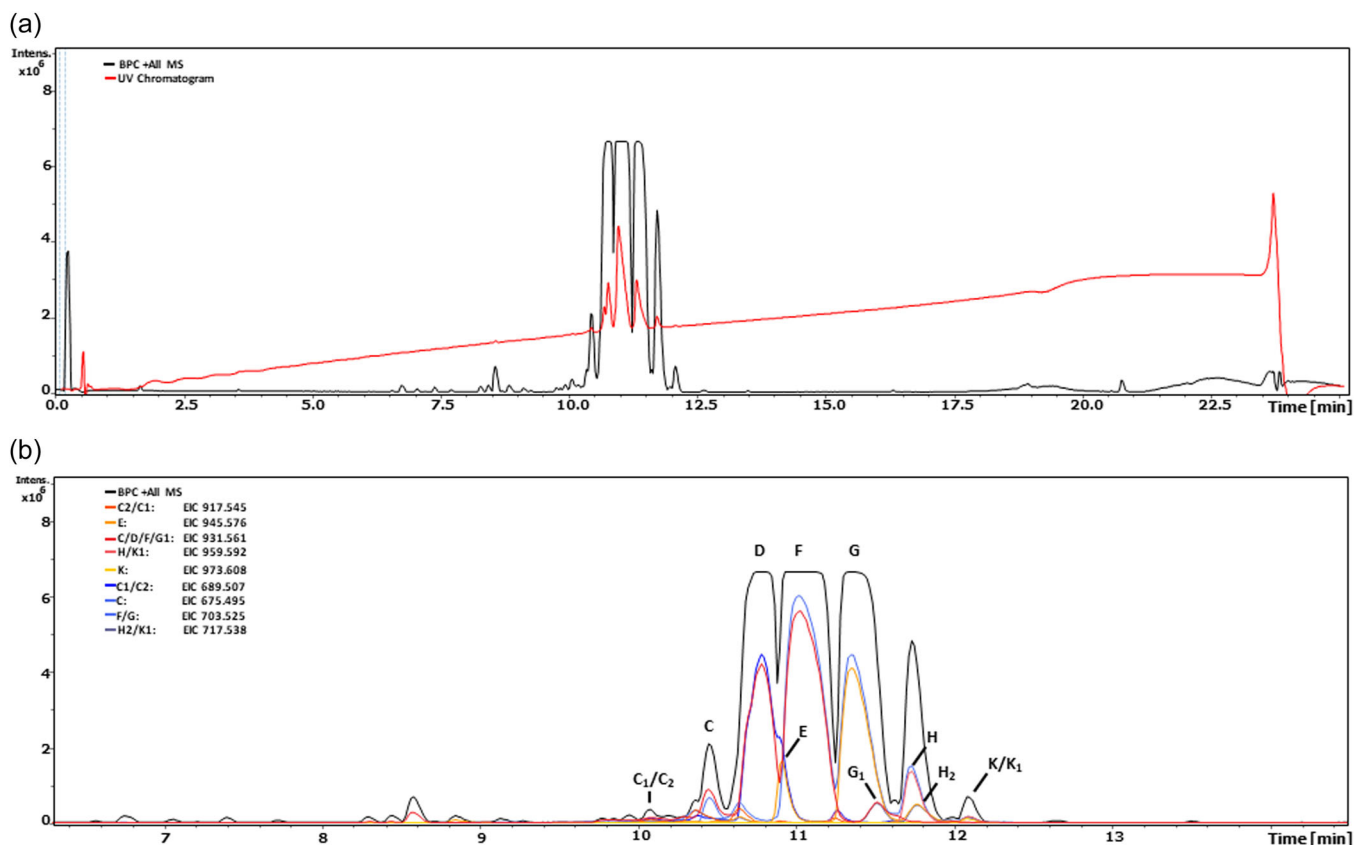


FIGURE 2 Ultra-high performance liquid chromatography coupled to high-resolution mass spectrometry (UHPLC-MS/MS) analysis of tolypin. (a) Overlay of UV/Vis chromatogram (red) and annotated base peak chromatogram (black). (b) Zoom-in from panel (a) in the window showing 7–14 min. Diagnostic γ_6 fragments (blue tones) and b_{10} fragments (red tones) of the mixture. The nomenclature of efrapeptins is based on literature. Additional information on all components can be found in Supporting Information S1: Tables S3–S11.

TABLE 2 General building scheme of tolypins and efrapeptins.

Position															
1	2	3	4	5	6	7	8	9	10	11	12	13	14	15	16
AcPip	Aib	Pip	Aib	Aib	Leu	β Ala	Gly	Aib	Aib	Pip	Aib	Gly	Leu	Iva	PIHPPE
			Iva	Iva				Iva			Iva	Ala		Aib	
				Ala											

Note: Conserved residues are highlighted in gray.

2.3 | Insecticidal effect of tolypin against *G. mellonella* larvae

The *in vivo* toxicity of drugs is usually characterized in preclinical rodent models, but invertebrate species, including larvae of the greater wax moth *G. mellonella*, have been introduced more recently to reduce the use of vertebrates in research.^[31] We tested the insecticidal effects of tolypin by injecting *G. mellonella* larvae, comparing the results against untreated negative controls, vehicle controls injected with 50% DMSO, and positive controls injected with 96% ethanol to trigger strong punctate melanization. Treatment with tolypin caused dose-dependent immediate paralysis from which the larvae did not recover. The effect of

the lowest concentration of 0.1 ng tolypin was indistinguishable from the DMSO control. However, there was no evidence of melanization following the injection of tolypin at any concentration, in contrast to the effect of ethanol, supporting the paralytic rather than the toxic effect of this peptaibiotic (Supporting Information S1: Figure S3). Our data agree with earlier studies reporting insecticidal effects in larvae and adults of various species.^[32] This may reflect the ability of efrapeptins and tolypins to inhibit vacuolar-type ATPase (V-ATPase) comparable to the effects of destruxin B, a well-characterized insecticidal cyclohexadepsipeptide.^[25,33] Destruxin B was also shown to inhibit the replication of hepatitis B viruses, which may help to explain the effect of tolypin against influenza viruses.^[34,35]

2.4 | Effect of tolypin against cultured mammalian cells

Tolypin (up to 10 ng/ μ L) reduced the viability of MDCK II cells by \leq 25% whereas 100 ng/ μ L tolypin triggered a highly cytotoxic effect (Figure 3a). We also used a trypan blue exclusion assay to assess whether tolypin has a cytostatic effect on MDCK II cells (Figure 3b). All cells were grown to confluency before treatment with tolypin, ionomycin as a positive control, or DMSO as a vehicle control for 48 h, with another set of cells left untreated, followed by the trypan blue assay to determine the total cell count compared with viable cells. Tolypin (up to 10 ng/ μ L) slightly reduced the total cell count compared with the untreated and DMSO controls but the number of viable cells was unchanged, indicating the inhibition of cell proliferation rather than cell death. In contrast, 100 ng/ μ L tolypin reduced the total cell count and the number of viable cells. Therefore, further investigations were conducted using tolypin at concentrations of 0.1, 1, and 10 ng/ μ L.

To gain insight into the metabolic changes triggered by the tolypin-dependent inhibition of F_1F_0 -ATP synthase, we analyzed the OCR and ECAR using the Agilent Seahorse XF96 system to detect changes in OXPHOS and glycolysis. The cells were tested using a MitoStress assay 48 h after the treatment (Figure 4a,b). Reagents were injected in the following order: oligomycin (1.58 μ g/ μ L), protonophore carbonyl cyanide-*p*-trifluoromethoxy phenylhydrazone (FCCP, 0.5 μ g/ μ L), a combination of rotenone (0.197 μ g/ μ L) and antimycin A (0.548 μ g/ μ L), and finally 2-deoxyglucose (2-DG, 8.2 g/L). Basal respiration was significantly reduced following treatment with tolypin or oligomycin compared with DMSO controls (Figure 4a.2). Oligomycin reduced the OCR by inhibiting ATP-synthase-linked respiration in both controls as expected. No change was observed in the cells pretreated with the ATP synthase inhibitors oligomycin (1.18 μ g/ μ L) and tolypin (0.1–10 ng/ μ L) compared to basal respiration (Figure 4a.2). FCCP causes the

collapse of the inner membrane proton gradient, activating the electron transport chain, and thus maximizing oxygen consumption. We found that tolypin and oligomycin triggered a concentration-dependent lower maximum respiration rate. The resulting respiratory capacity was significantly lower for all cells treated with ATP synthase inhibitors compared with DMSO controls (Figure 4a.3). Finally, antimycin A and rotenone shut down the electron transport chain, leaving nonmitochondrial respiration as the only energy source. Here, pretreatment with the ATP synthase inhibitors resulted in the inhibition of nonmitochondrial respiration compared to controls. Finally, 2-DG (which inhibits glycolysis) did not affect the OCR in samples treated with the ATP synthase inhibitors, suggesting that the main effect is due to the inhibition of mitochondrial respiration. Tolypin treatment also increased the basal ECAR at all concentrations tested (Figure 4b). For treatments with 0.1 and 1 ng/ μ L tolypin, no significant changes in the ECAR were observed after the injection of oligomycin and FCCP, suggesting that glycolytic reserves were absent and the cells therefore relied solely on glycolysis.

Next, we measured changes in the OCR and ECAR directly after the injection of ATP synthase inhibitors (Figure 4c,d). Reagents were injected in the following order: tolypin (0.1, 1, or 10 ng/ μ L) or the control oligomycin (1.18 μ g/ μ L), FCCP (0.5 μ g/ μ L), a combination of rotenone (0.197 μ g/ μ L) and antimycin A (0.548 μ g/ μ L), and 2-DG (8.2 g/L). Again, oligomycin and 10 ng/ μ L tolypin reduced the OCR, but lower concentrations of tolypin did not immediately affect the OCR. The same trend was observed for the ECAR, where an increase was observed following treatment with oligomycin and the highest concentration of tolypin, whereas 0.1 and 1 ng/ μ L tolypin had no effect compared with the controls. Only the highest concentration of tolypin influenced the maximal respiratory capacity, which was determined following the application of FCCP. These results indicate a concentration- and time-dependent effect, probably due to diffusion and transport processes.

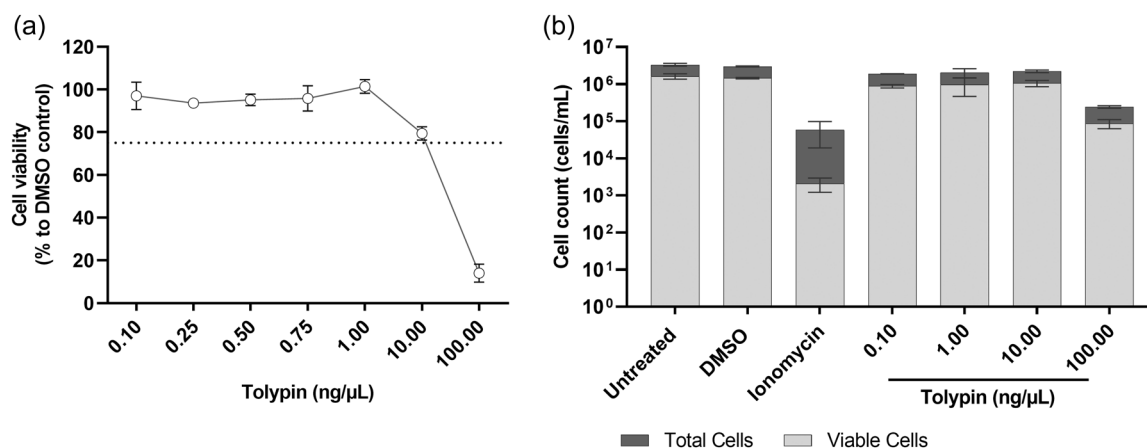


FIGURE 3 Effect of tolypin on MDCK II cell viability and proliferation. (a) Cell viability in the presence of tolypin after 48 h assessed using the CellTiter-Glo assay. The cell viability was normalized to the dimethyl sulfoxide (DMSO) control, which was set to 100%. The dotted line represents the cut-off value of 25% cytotoxicity. (b) Trypan blue exclusion assay in confluent cells after exposure to tolypin for 48 h. Data are means \pm SD of $n = 3$ –6 independent measurements.

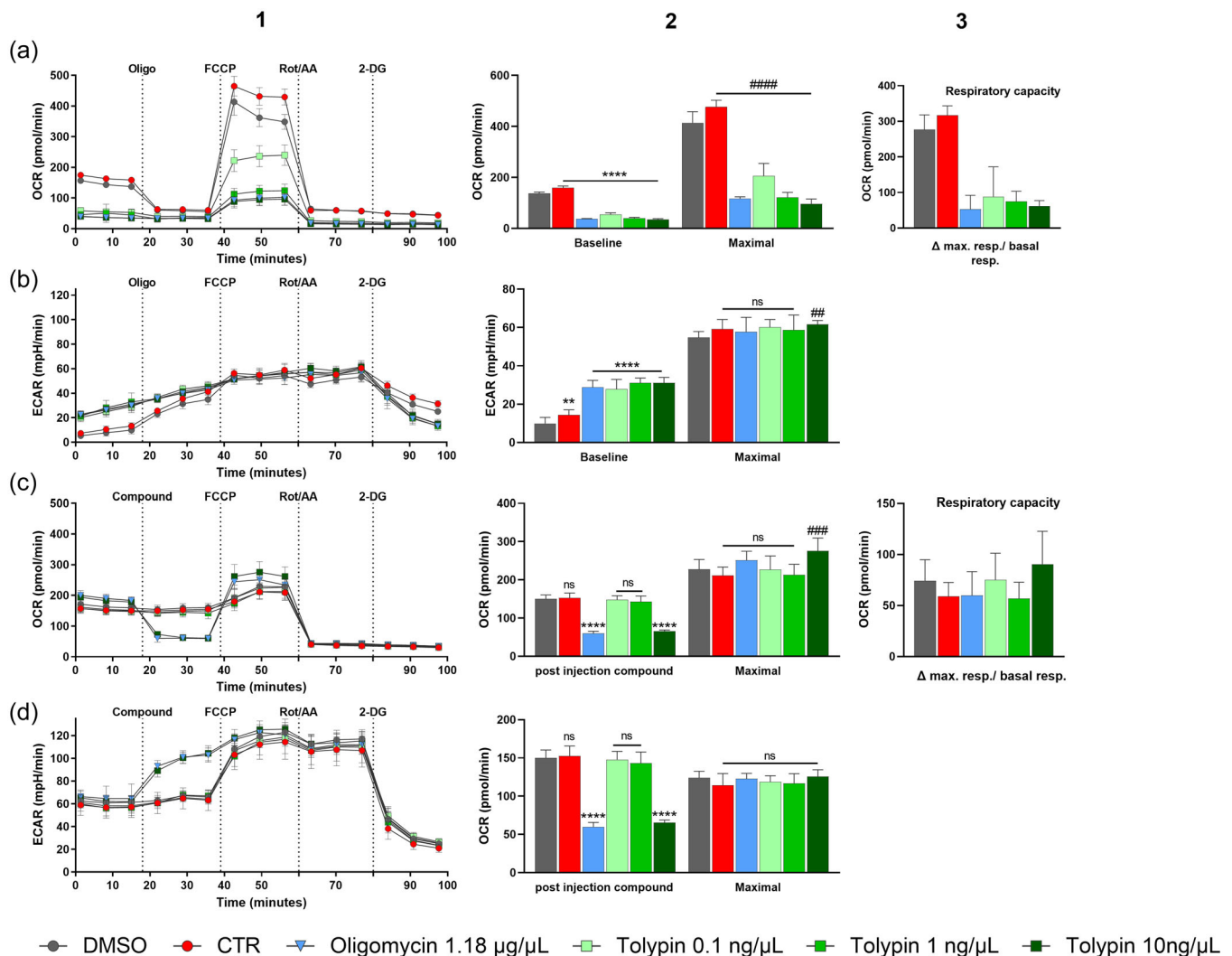


FIGURE 4 The oxygen consumption rate (OCR) and extracellular acidification rate (ECAR) in MDCK II cells in response to tolypin. (a, b) Cells were treated for 48 h with different concentrations of tolypin or the control oligomycin (1.18 µg/µL), or (c, d) measurements were taken directly after injection. We then injected modulators of the respiratory chain and glycolysis: oligomycin (Oligo) 1.58 µg/µL, cyanide-*p*-trifluoromethoxy phenylhydrazine (FCCP) 0.5 µg/µL, rotenone (Rot.) 0.197 µg/µL and antimycin A (AA) 0.548 µg/µL, and 2-deoxyglucose (2-DG) 8.2 g/L. Data are means ± SD of $n = 8$ –12 independent measurements. Statistical significance was calculated by two-way analysis of variance (ANOVA) for multiple comparison versus vehicle control (DMSO): ** $p < 0.01$, *** $p < 0.001$ and **** $p < 0.0001$ for baseline; # $p < 0.01$, ## $p < 0.001$ and ### $p < 0.0001$ for maximal respiration.

ATP synthase is required for energy generation, and inhibition therefore has serious consequences in terms of homeostasis and metabolism. The MDCK II cells tolerated up to 10 ng/µL tolypin (Figure 3a). The metabolic switch in MDCK II cells seems to trigger only slight cytostatic effects (Figure 3b). A previous study using human umbilical vein endothelial cells (HUVECs) suggested that tolypin is unable to cross the cell membrane and therefore only inhibits nonmitochondrial ATP synthase on the cell surface.^[36] By using the Seahorse system, we showed that the OXPHOS machinery is impaired after tolypin treatment and conclude that tolypin does have a direct impact on mitochondrial ATP synthase (Figure 4), suggesting that tolypin is taken up into the cell and trafficked to the mitochondria.

2.5 | Antiviral effect of tolypin

Next, we investigated the antiviral effect of tolypin at concentrations of 0.1, 1, and 10 ng/µL by measuring the CPE of four viral strains in MDCK II cells 48 h postinfection. IBV Malaysia/B and Massachusetts/B were inhibited more efficiently by 1 ng/µL than 10 ng/µL tolypin, probably reflecting the higher cytotoxicity of the larger dose (Figure 5a). At a concentration of 1 ng/µL, tolypin showed an antiviral activity of 56.9% against Malaysia/B and 69.1% against Massachusetts/B. Marginal antiviral activity against H3N2 was observed at 13.7%, but H1N1pdm was not inhibited by tolypin treatment. To confirm that the effect on virus replication was due to the inhibition of F_1F_0 -ATP synthase, we used oligomycin as a control (Figure 5b).

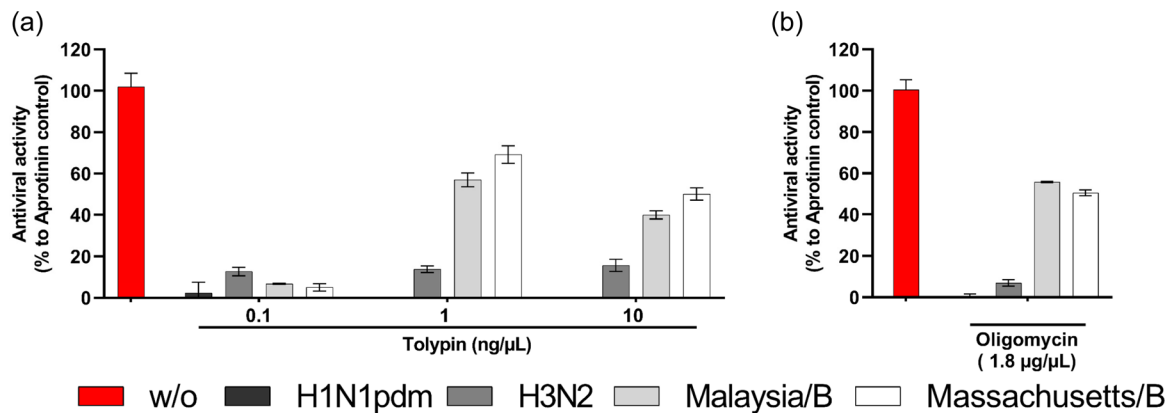


FIGURE 5 Antiviral activity of tolypin against diverse influenza virus strains in MDCK II cells. The cells were left untreated (w/o) or were infected at a multiplicity of infection (MOI) of 1 for H1N1pdm, H3N2, and Malaysia/B, or at an MOI of 0.01 for Massachusetts/B and were incubated for 1 h before treatment with (a) the indicated concentrations of tolypin or (b) 1.18 μg/μL oligomycin. After 48 h, a CellTiter-Glo assay was used to determine cell viability. Raw luminescence values were baseline-corrected to the virus control and normalized to the 651 ng/μL aprotinin positive control set to 100%. Data are means ± SD of $n = 3$ independent measurements.

The inhibition of viral replication by oligomycin showed a similar trend to tolypin even though the two reagents act on different target sites of the F_1F_o -ATP synthase.^[37] Again, the effect was strongest against the IBV strains, weaker against H3N2, and negligible against H1N1pdm. The antiviral activity of the Malaysia/B and Massachusetts/B strains was 55.6% and 50.3%, respectively, whereas the observed antiviral activity against H3N2 was only 6.9%.

Given the difference in efficacy observed when inhibiting IAV and IBV strains, we tested tolypin and oligomycin against four other strains to determine whether the effect was consistent (Supporting Information S1: Figure S4). We observed the strong inhibition of two additional IBV strains (B/Brisbane/60/2008 and B/California/12/2015). Tolypin and oligomycin showed similar levels of antiviral activity against Brisbane/B by similar amounts (57.2% and 56.4%, respectively). Likewise, the reagents similarly also showed an antiviral activity against California/B (52.5% and 51.2%, respectively). Tolypin also inhibited both additional IAV strains but was less efficacious. The antiviral activity against A/swine/Wisconsin/1/67 (Wisconsin/H1N1) was 14.1% and the against A/Puerto Rico/8/34 (PR8) was 31.7%.

Given the differential efficacy of ATP-synthase inhibitors in the IAV and IBV backgrounds, we assessed the effect of tolypin and oligomycin on multicycle viral replication (Figure 6). Samples of supernatant from the MDCK II cell cultures were taken at various time points and the viral titer was determined using a plaque assay. H1N1pdm multicycle replication was unaffected by the inhibitors (Figure 6a), whereas H3N2 titers were reduced by 2 log units by tolypin and oligomycin, but recovered to pretreatment levels after 24 and 32 h, respectively (Figure 6b). This agrees with the 3 log unit reduction reported for IAV strain SC35M in A549 in human lung cells after oligomycin treatment.^[21] In contrast, the replication of IBV Malaysia/B and Massachusetts/B was significantly inhibited by tolypin treatment, resulting in a titer reduction of 4–5 log units compared to viral replication in the untreated control cells (Figure 6c,d).

The inhibition of F_1F_o -ATP synthase efficiently blocked the replication of IBV but had a weaker effect against IAV, and this was consistent regardless of the specific target site of the inhibitor (Figures 5 and 6). Virus replication is an energy-demanding process involving stages of viral uptake, intracellular transport, genome replication, transcription, translation, assembly, genome packaging, and budding.^[38] Influenza typically consumes 1% of the total energetic budget of a eukaryotic cell during the course of an infection, in part by inducing metabolic changes such as increasing the rate of glycolysis and glutaminolysis.^[21,39,40] Given that cells switch completely to glycolysis following tolypin treatment to meet their energy demands, this may interfere with virus-induced metabolic reprogramming. Therefore, we propose that the IAV and IBV strains differ in their ability to redirect cellular energy resources to virus replication. Although F_1F_o -ATPase was originally thought to be present only in the mitochondria, this view has changed over the last 30 years following the detection of F_1F_o -ATPases at the plasma membrane in several cell types, including hepatocellular carcinoma cells (HepG2), HUVECs, and A549 cells.^[41] Plasma membrane F_1F_o -ATP synthase is required for influenza virus production and budding in HEK 293 cells, whereas the mitochondrial F_1F_o -ATP synthase is not.^[42] The budding of IAV strain WSN from MDCK II cells can also be suppressed by the depletion of ATP.^[43]

2.6 | Quantification of glucose and lactate in cell supernatant after infection

The treatment of cells with OXPHOS inhibitors such as tolypin forces the cells to switch to other pathways to meet their energy demands, including glycolysis. Additionally, infection with influenza viruses increases the energy demand. We therefore, monitored glucose consumption and lactate formation in the presence and absence of tolypin in MDCK II cells infected with the H1N1pdm or Malaysia/B strains (and in uninfected controls) over a period of 32 h (Figure 7).

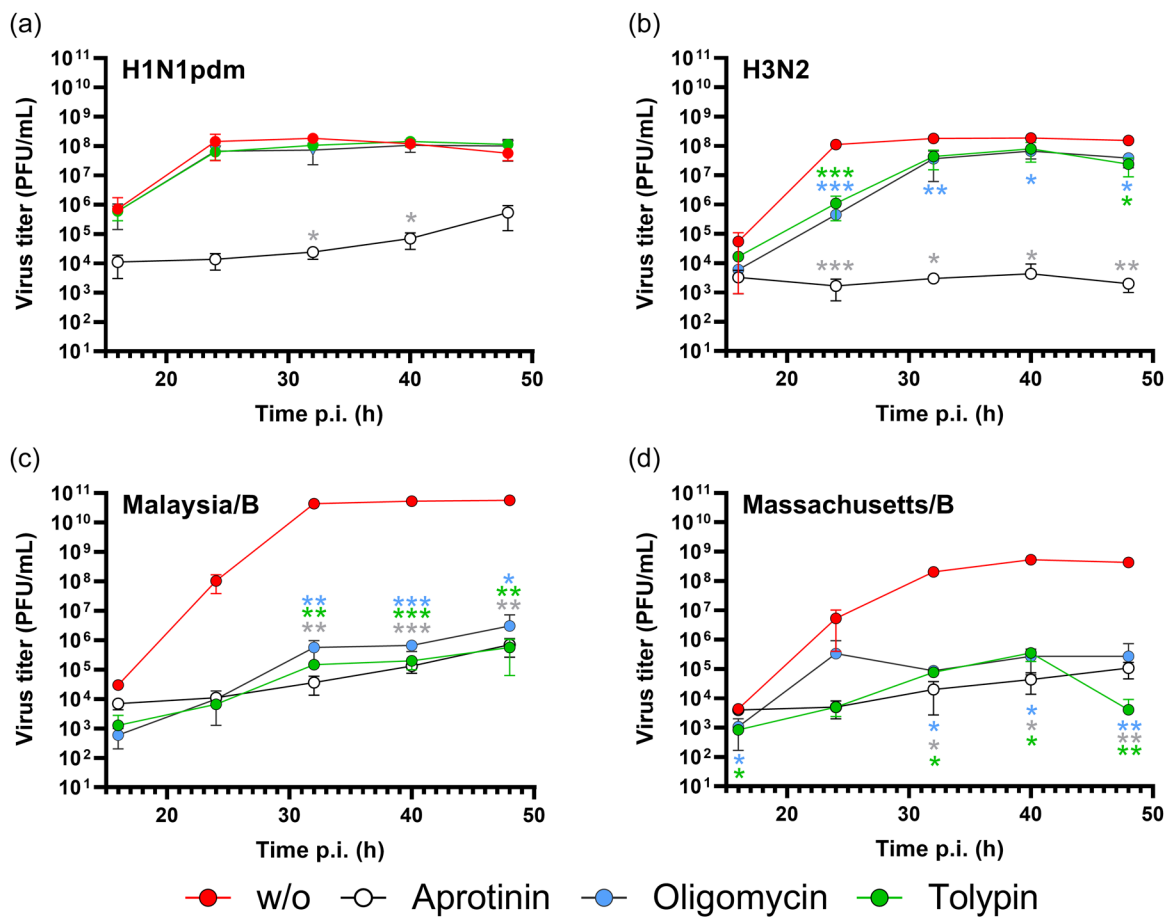


FIGURE 6 Multicycle replication of influenza virus strains in tolypin-treated MDCK II cells. The cells were inoculated with (a) H1N1pdm, (b) H3N2, (c) Malaysia/B, or (d) Massachusetts/B at a multiplicity of infection (MOI) of 0.001 for 1 h before exposure to 1 ng/ μ L tolypin, 1.18 μ g/ μ L oligomycin or 325 ng/ μ L aprotinin (plus controls without further treatment, w/o). Cell supernatants were collected and viral titers presented as plaque-forming units (PFU)/mL were determined by plaque assay. Data are means \pm SD of $n = 3$ independent measurements. Statistical significance was determined by two-way analysis of variance (ANOVA) for multiple comparison versus the untreated group (* $p < 0.1$, ** $p < 0.01$, and *** $p < 0.001$).

As expected, LC-MS analysis revealed lower glucose levels in the supernatant of cells treated with 1 ng/ μ L tolypin compared with untreated controls (Figure 7a). Infection with H1N1pdm or Malaysia/B also led to an increase in glucose consumption, but this was less pronounced compared with the tolypin treatment. The tolypin-treated samples that were also infected showed similar increases in glucose consumption compared with the tolypin-treated control. In the case of lactate, we observed no differences between infected samples and controls (Figure 7b). The highest lactate concentrations were found in tolypin-treated cells infected with Malaysia/B. Slightly lower lactate concentrations were detected in the tolypin-treated cells and those infected with H1N1pdm. The metabolic switch was therefore accompanied by changes in glucose consumption and lactate production but there were no differences between the virus-infected and control cells (Figure 7). The stability of H1N1pdm and Malaysia/B at low pH was investigated to ensure that the inhibition of virus replication was not due to lactate-dependent pH changes in the medium (Supporting Information S1: Figure S5). We observed no reduction in the viral titers in the pH

range 5.5–8. The differential inhibition of IAV and IBV replication is therefore not due to pH stability.

Previous studies investigating metabolic changes in response to influenza virus infection considered different strains to the ones we used in our study and focused on later postinfection time points, which are more likely to reflect the impact of apoptosis than the viral infection.^[40] Importantly, all the previous studies cited above solely considered IAV strains and no further data are available for IBV strains. Our data therefore suggest there are differences between IAV and IBV strains in terms of the capacity to reprogram cellular metabolism, and this should be investigated in more detail.

3 | CONCLUSION

New lead structures are needed to develop promising therapeutic options for the treatment of influenza virus infections. Interfering with the cell's energy metabolism offers novel targets for antiviral therapies. We have described the chemical characteristics and

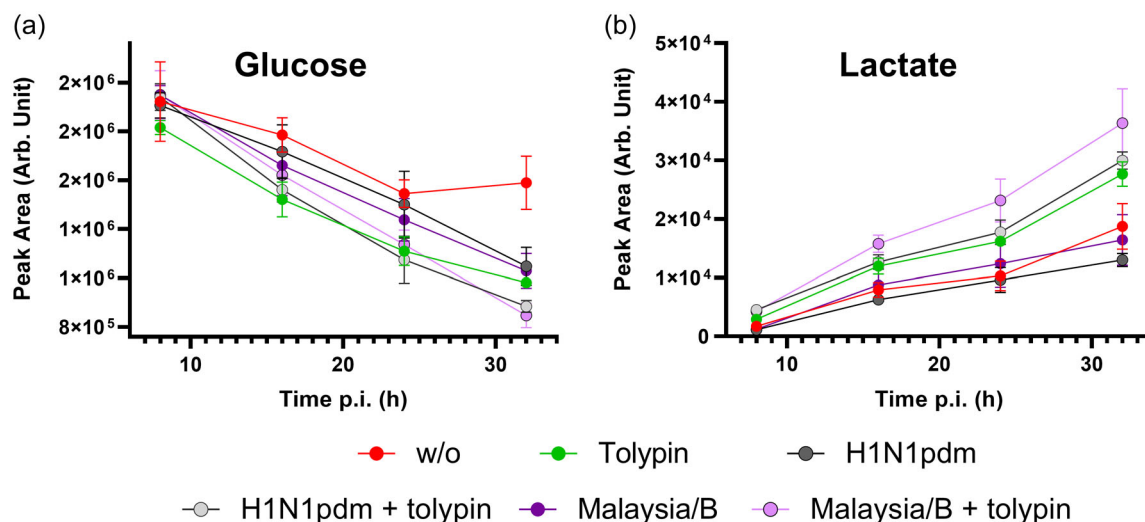


FIGURE 7 Glucose consumption and lactate formation in MDCK II cells infected with H1N1pdm or Malaysia/B and the effect of treatment with 1 ng/ μ L tolypin. Confluent MDCK II cells were infected or left uninfected and then treated with tolypin or left untreated. At given time points, supernatants were collected for the measurement of (a) glucose and (b) lactate concentrations by LC-MS/MS. Data are means \pm SD of $n = 3$ independent biological replicates, measured in technical triplicates.

antiviral activity of tolypin. The inhibition of ATP synthase by tolypin reduces OXPHOS activity in MDCK II cells, forcing a switch to glycolysis to maintain an energy supply. Tolypin did not inhibit the replication of H1N1pdm but reduced the titers of several IBV strains by up to 5 log units after 32 h. We present the first example of UHPLC-isCID-HR-MS/MS data for the characterization of tolypins as typical 16-residue efrapeptin-type peptaibiotics, confirming the suitability of this method for the sequencing and structural elucidation of partially co-eluting fungal peptides. Due to recent changes in the phylogeny and systematics of the genus *Tolypocladium*, a reinvestigation of the peptaibiotic profiles (including efrapeptin-type peptaibiotics) of the currently accepted 48 species would contribute to progress in chemotaxonomy and facilitate the detection of novel bioactive natural products. Our results also highlight the need for further studies to identify specific differences between IAV and IBV to develop targeted treatments for influenza virus infections.

4 | EXPERIMENTAL

4.1 | Chemistry

4.1.1 | General

Information about the five peptaibiotics used in this study is provided in Table 3. Antimycin A, carbonyl cyanide-*p*-trifluoromethoxyphenylhydrazone (FCCP), 2-desoxy-D-glucose (2-DG), ionomycin, permethrin, and rotenone were purchased from Sigma-Aldrich/Merck. The serine protease inhibitor aprotinin and disodium adenosine 5'-triphosphate (ATP) were obtained from Carl Roth. Oligomycin A was obtained from Cayman Chemicals. LC-MS

grade chemicals and solvents for mass spectrometry were sourced from VWR International and Thermo Fisher Scientific.

4.1.2 | Mass spectrometry

Ultrahigh performance liquid chromatography coupled to quadrupole time-of-flight high-resolution mass spectrometry and MS/MS analysis was carried out using an Agilent 1290 Infinity LC system coupled to a QTOF maXis II mass spectrometer (Bruker Daltonics) equipped with an ESI source. Samples were loaded onto a Acquity UPLC BEH C18 column (130 \AA , 1.7 μ m, 2.1 \times 100 mm) equipped with the appropriate pre-column (130 \AA , 1.7 μ m, 2.1 \times 5 mm) at 45°C and fractions were eluted using a linear gradient of buffers A (0.1% formic acid in water) and B (0.1% formic acid in acetonitrile). The following gradient was applied at a flow rate of 0.6 mL/min: 0 min/95% A, 0.30 min/95% A, 18.00 min/4.75% A, 18.10 min/0% A, 22.50 min/0% A, 22.60 min/95% A, 25.00 min/95% A. Data were acquired in the scan range 50–2000 m/z at 1 Hz. MS/MS analysis was carried out at 6 Hz and the top five most intense ions in each full mass spectrum were targeted for collisional induced dissociation (CID) using N_2 (Supporting Information S1: Table S12). Precursors were excluded after two spectra, released after 0.5 min, and reconsidered if the intensity of an excluded precursor increased by ≥ 1.5 -fold. Targeted MS/MS analysis was applied to all y_6 ions with in-source CID energy of 20 eV and collision energy of 48 and 60 eV (combined).

4.1.3 | LC-MS-based approximation of relative abundancies

Extracted ion chromatograms (± 0.02 Da) from diluted samples were generated for the comparison of peak areas. Independent analysis

TABLE 3 Peptaibiotics investigated in this study.

Substance	Batch No.	No. of peptides	Length	Source
Alamethicin F50	#2 (K8/87)	13	20	<i>Trichoderma arundinaceum</i> CBS 123793 (=NRRL 3199) ^a
Antiamoebin	#AAM6K3	9	16	<i>Emericellopsis fimetaria</i> CBS 176.60 (=ATCC 16540 = IMI 081600 = MUCL 11495; syn. <i>Stilbella fimetaria</i> , syn. <i>Emericellopsis synnematicola</i>)
Paracelsin	#HB1	8	20	<i>Trichoderma reesei</i> CBS 392.92 (=QM 9414 = ATCC 26921)
Trichotoxin A-40	#151085	6	18	<i>Trichoderma asperellum</i> CBS 361.97 (=NRRL 5242) ^b
Tolypin	#Jegorov 150890 ^[20]	12	16	<i>Tolyocladium inflatum</i> IE 1897

^aOriginally identified as *Trichoderma viride*.

^bOriginally identified as *Trichoderma viride*.

was applied to the first and second isotope of the y_6 and b_{10} fragments. Used extracted ion chromatograms and resulting peak areas are given in Supporting Information S1: Table S13. The detector remained in the linear range.

4.2 | Biological assays

4.2.1 | Insecticidal activity of tolypin against *G. mellonella*

The in vivo toxicity of drugs is typically assessed using preclinical rodent models. However, to minimize the use of vertebrates in research, invertebrate species such as the larvae of the greater wax moth *G. mellonella* have recently been introduced. We randomly selected 20 last-instar *G. mellonella* larvae (Tropic Shop) per treatment, each individual weighing 500 ± 50 mg. Larvae with signs of melanization were excluded. Tolypin was dissolved in 50% DMSO at a concentration of $10 \text{ ng}/\mu\text{L}$, and $5 \mu\text{L}$ of the solution was injected into the hemocoel through an anterior proleg using a manual microsyringe pump (World Precision Instruments) equipped with a Braun Omnican F syringe (1 mL , 30 G , $0.3 \times 12 \text{ mm}$). Control larvae were untreated or injected with either $5 \mu\text{L}$ 50% DMSO as a vehicle control or $10 \mu\text{L}$ 96% ethanol (Carl Roth) to provoke melanization. The larvae were incubated at $22 \pm 2^\circ\text{C}$ in the dark for 11 days. Melanization and mortality were recorded daily. Larvae were considered dead if we observed signs of punctate or systemic melanization or prolonged absence of movement (irreversible paralysis). The rates of survival, pupation, and metamorphosis were evaluated using GraphPad Prism v9.1.2 (GraphPad Software).

4.2.2 | Cell culture

Madin-Darby canine kidney II (MDCK II) cells were maintained in Dulbecco's modified Eagle's medium (DMEM) GlutaMAX supplemented with 10% fetal calf serum (FCS) and 1% penicillin/streptomycin (all media and supplements from Thermo Fisher Scientific). The cells were incubated at 37°C in a 5% CO_2 atmosphere.

4.2.3 | Cytotoxicity screening in cell culture

Cells were seeded in 96-well plates and incubated at 37°C in a 5% CO_2 atmosphere until they reached 90% confluence. They were then treated with tolypin, ionomycin, or DMSO. The peptaibiotics were dissolved in DMSO ($10 \mu\text{g}/\mu\text{L}$ stock) and further diluted with DMSO as required. Ionomycin was also dissolved in DMSO ($7.47 \mu\text{g}/\mu\text{L}$, final dilution $74.74 \text{ ng}/\mu\text{L}$). The final DMSO concentration was 1% (v/v). The plates were incubated as above for 48 h and cell viability was assessed by measuring the ATP content using the CellTiter-Glo Luminescent Cell Viability assay (Promega) according to the manufacturer's instructions. Luminescence was recorded using black 96-well plates in a Synergy H4 microplate reader (Biotek/Agilent). The luminescence readings were normalized to the DMSO control, which was set to 100% cell viability.

4.2.4 | Live and dead cell count assay

Cells were seeded in 24-well plates and incubated as above until they reached 90% confluence. They were then treated with tolypin at concentrations of 0.1, 1, and $10 \text{ ng}/\mu\text{L}$, $7.47 \mu\text{g}/\mu\text{L}$ ionomycin or 1% DMSO as a vehicle control. The plates were incubated as above for 48 h and then the cells were detached using $200 \mu\text{L}$ TrypLE (Thermo Fisher Scientific) and resuspended in DMEM. Aliquots of $15 \mu\text{L}$ were mixed 1:1 with trypan blue solution (Merck) to give a final trypan blue concentration of 0.2% before transferring this solution to cell-counting slides and recording the number of living and dead cells in a BioRad TC20 Automated Cell Counter.

4.2.5 | Measurement of OCR and ECAR

The OCR and ECAR of MDCK II cells were measured in the presence and absence of tolypin using the XF Cell Mito Stress Kit on a Seahorse XF96 system (Agilent) according to the manufacturer's instructions. Briefly, MDCK II cells were seeded in 96-well XF plates

(Agilent) and incubated at 37°C in a 5% CO₂ atmosphere for 24 h. The cells were then treated with tolypin (0.1, 1, or 10 ng/μL) or the control oligomycin (1.18 μg/μL) 48 h before measuring the long-term effect on OCR and ECAR, or the same reagents and concentrations were injected via the first port (slot A) to measure the acute impact. The cells were washed once with 100 μL medium, which was then replaced with 180 μL of Seahorse assay medium (DMEM containing 25 mM D-glucose, 2 mM L-alanyl-L-glutamine, 1 mM sodium pyruvate, pH 7.35). We then injected modulators of energy metabolism as follows: 1.58 μg/μL oligomycin, 0.5 μg/μL FCCP, 0.197 μg/μL rotenone, 0.548 μg/μL antimycin A, and 8.2 μg/μL 2-DG. Following the application of each substance and mixing for 3 min, each measurement was recorded for 3 min in triplicate.

4.2.6 | Viruses

The influenza viruses used in this study were strains A/Hamburg/05/2009 (H1N1pdm), A/Hessen/1/2003 (H3N2), A/PuertoRico/8/34 (PR8), A/swine/Wisconsin/1/67 (H1N1), B/Malaysia/2506/2004 (Malaysia/B), B/Massachusetts/71 (Massachusetts/B), B/Brisbane/60/2008 (Brisbane/B), and B/California/12/2015 (California/B). The viruses were propagated in MDCK II cells with infection medium (DMEM GlutaMAX) supplemented with 0.2% bovine serum albumin (bovine serum albumin [BSA], Carl Roth), 1% penicillin/streptomycin and 1 μg/mL bovine N-tosyl-L-phenylalanine chloromethyl ketone (TPCK)-treated trypsin (Thermo Fisher Scientific) at a multiplicity of infection (MOI) of 0.001–1. After 48 h, cell supernatants were cleared by centrifugation (2000 x g, 10 min, 4°C) and stored at –80°C.

4.2.7 | Screening of antiviral activity in MDCK II cells

MDCK II cells were inoculated with selected viruses at a MOI of 0.01, 0.1, or 1 to cause a significant CPE after 48 h. For H1N1pdm, PR8, H1N1, H3N2, Malaysia/B, Brisbane/B, and California/B we used a MOI of 1 and for Massachusetts/B the MOI was 0.01. Confluent MDCK II cells were inoculated with the virus in the infection medium. After incubation for 1 h, the cells were washed twice with phosphate-buffered saline (PBS), followed by treatment with various concentrations of tolypin (0.1–100 ng/μL) or 651 ng/μL aprotinin (65.11 mg/mL stock in water) as a control in infection medium supplemented with 1 μg/mL bovine TPCK-treated trypsin. Aprotinin prevents proteolytic activation and multiplication of influenza viruses in cell culture and rodents and therefore serves as a positive control for inhibition of viral replication.^[28] After incubation for 48 h at 37°C in a 5% CO₂ atmosphere, cell viability was determined using the CellTiter-Glo assay as described above. Luminescence values were subtracted from the blank (virus-treated cells) before normalizing to the aprotinin control, which was set to 100% antiviral activity.

4.2.8 | Multicycle replication in MDCK II cells

MDCK II cells were seeded in 24-well plates and grown to 100% confluence. The cells were inoculated with the virus at a MOI of 0.001 in the infection medium. After incubation for 1 h at 37°C in a 5% CO₂ atmosphere, the cells were washed twice with PBS, followed by treatment with tolypin, oligomycin, or aprotinin as a control in an infection medium supplemented with 1 μg/mL TPCK-treated trypsin. Supernatants were collected 16, 24, 32, 40, and 48 h postinfection and viral titers were determined by plaque assay.

4.2.9 | Stability of H1N1pdm and Malaysia/B as a function of pH

To determine the stability of H1N1pdm and Malaysia/B as a function of pH, virus suspensions were incubated in buffers across a pH range of 5–7.5 for 30 min. Afterwards, serial dilutions were used to determine the viral titer by plaque assay.

4.2.10 | Plaque assay in MDCK II cells

MDCK II cells were seeded in 24-well plates and grown to confluence. Samples from the multicycle replication experiments were serially diluted in an infection medium and used to inoculate the cells. After incubation for 1 h at 37°C in a 5% CO₂ atmosphere, the cells were washed twice with PBS and then overlaid with 1.25% Avicel in MEM (both Thermo Fisher Scientific) supplemented with 0.3% BSA, 1% glutamine, and 1% penicillin/streptomycin. The overlay medium was removed after 48 h and the cells were washed with PBS, fixed with 4% paraformaldehyde (Carl Roth) and plaques were visualized by 0.25% crystal violet staining (Carl Roth). Titers were calculated from the number of plaques, expressed as plaque-forming units PFU/mL.

4.2.11 | Quantification of glucose and lactate in the cell supernatant

MDCK II cells were infected with viruses as described above. Supernatant samples (50 μL) were collected 0, 8, 16, 24, and 30 h postinfection and transferred to a second centrifuge tube containing 100 μL 0.1% formic acid in acetonitrile. The solution was centrifuged (3622 x g, 5 min, 4°C) to pellet the precipitated proteins and 10 μL of the supernatant was diluted with 990 μL 0.1% formic acid in water for MS analysis using the QTOF maXis II instrument as described above (see Section 4.1.2). Parameters for extracted ion chromatograms were extracted ion chromatogram (EIC) 91.0385 ± 0.01 for lactate and EIC 203.0526 ± 0.01 for glucose. The results were analyzed using Compass DataAnalysis v5.3 (Bruker).

4.2.12 | Statistical analysis

All data are presented as means \pm standard deviations (SD). Normality was determined using the Shapiro–Wilks W test before two-way analysis of variance (ANOVA) for multiple comparisons. If assumptions of normality were not met, a Kruskal–Wallis test was applied, followed by Dunn's post hoc test. The data were visualized using GraphPad Prism 9.1.2.

ACKNOWLEDGMENTS

The authors thank Stephanie Schlimbach for valuable technical support and Katharina Elsässer for technical assistance with the Seahorse experiments. The authors gratefully acknowledge the comments of Dr. Gerard Verkleij (Westerdijk Fungal Biodiversity Institute, Utrecht, Netherlands) and Dr. Andrey Yurkov (DSMZ-German Collection of Microorganisms and Cell Cultures GmbH, Braunschweig, Germany) on the taxonomy of the peptaibiotic-producing strains listed in Table 3. The authors thank Dr. Richard M Twyman for manuscript editing. This research was funded by the German Federal Ministry for Education and Research (BMBF) under the ASCRIBE program (grant number 01KI2024). Open Access funding enabled and organized by Projekt DEAL.

CONFLICTS OF INTEREST STATEMENT

The authors declare no conflicts of interest.

DATA AVAILABILITY STATEMENT

Raw UHPLC-MS/MS data in Bruker and mzML format for tolypin supporting the findings of this study are available here: <https://doi.org/10.24406/fordatis/356>.

ORCID

Johanna Eichberg  <http://orcid.org/0009-0000-3172-1036>
 Markus Oberpaul  <https://orcid.org/0000-0002-6860-8173>
 Christoph Hartwig  <http://orcid.org/0000-0003-2050-9579>
 Andrea Helga Geißler  <http://orcid.org/0009-0003-8831-5073>
 Carsten Culmsee  <https://orcid.org/0000-0002-5121-5015>
 Andreas Vilcinskas  <https://orcid.org/0000-0001-8276-4968>
 Eva Böttcher-Friebertshäuser  <https://orcid.org/0000-0002-0007-8110>
 Hans Brückner  <https://orcid.org/0000-0003-4743-7587>
 Thomas Degenkolb  <https://orcid.org/0000-0002-7592-8300>
 Kornelia Harges  <http://orcid.org/0009-0000-1670-7383>

REFERENCES

- [1] WHO, *Influenza (Seasonal)* **2023**, [https://www.who.int/news-room/fact-sheets/detail/influenza-\(seasonal\)](https://www.who.int/news-room/fact-sheets/detail/influenza-(seasonal)) (accessed: May 2024).
- [2] J. Eichberg, E. Maiworm, M. Oberpaul, V. Czudai-Matwich, T. Lüddecke, A. Vilcinskas, K. Harges, *Viruses* **2022**, *14*, 2452.
- [3] T. Degenkolb, H. Brückner, *Chem. Biodiversity* **2008**, *5*, 1817.
- [4] B.-S. Yun, I.-D. Yoo, Y. H. Kim, Y.-S. Kim, S.-J. Lee, K.-S. Kim, W.-H. Yeo, *Tetrahedron Lett.* **2000**, *41*, 1429.
- [5] Y. Luo, D.-D. Zhang, X.-W. Dong, P.-B. Zhao, L.-L. Chen, X.-Y. Song, X.-J. Wang, X.-L. Chen, M. Shi, Y.-Z. Zhang, *FEMS Microbiol. Lett.* **2010**, *313*, 120.
- [6] K. Kai, K. Mine, K. Akiyama, S. Ohki, H. Hayashi, *J. Pestic. Sci.* **2018**, *43*, 283.
- [7] R. O. Fox, F. M. Richards, *Nature* **1982**, *300*, 325.
- [8] H. Duclouhier, Y. Pichon, *Eur. Biophys. J.* **2004**, *33*, 169.
- [9] J. Kirschbaum, C. Krause, R. K. Winzheimer, H. Brückner, *J. Pept. Sci.* **2003**, *9*, 799.
- [10] G. Irmscher, G. Bovermann, G. Boheim, G. Jung, *Biochim. Biophys. Acta* **1978**, *507*, 470.
- [11] A. Jaworski, H. Brückner, *J. Chromatogr. A* **1999**, *862*, 179.
- [12] H. Brückner, H. Graf, M. Bokel, *Experientia* **1984**, *40*, 1189.
- [13] P. A. Grigoriev, B. Schlegel, M. Kronen, A. Berg, A. Härtl, U. Gräfe, *J. Pept. Sci.* **2003**, *9*, 763.
- [14] M. J. Thirumalachar, *Hind. Antibiot. Bull.* **1968**, *10*, 287.
- [15] H. Duclouhier, C. F. Snook, B. A. Wallace, *Biochim. Biophys. Acta Biomemb.* **1998**, *1415*, 255.
- [16] A. Jaworski, H. Brückner, *J. Pept. Sci.* **2000**, *6*, 149.
- [17] S. Skalickova, Z. Heger, L. Krejcova, V. Pekarik, K. Bastl, J. Janda, F. Kostolansky, E. Vareckova, O. Zitka, V. Adam, R. Kizek, *Viruses* **2015**, *7*, 5428.
- [18] M. B. Uddin, B.-H. Lee, C. Nikapitiya, J.-H. Kim, T.-H. Kim, H.-C. Lee, C. G. Kim, J.-S. Lee, C.-J. Kim, *J. Microbiol.* **2016**, *54*, 853.
- [19] J. P. Abrahams, S. K. Buchanan, M. J. van Raaij, I. M. Fearnley, A. G. Leslie, J. E. Walker, *Proc. Natl. Acad. Sci. U.S.A.* **1996**, *93*, 9420.
- [20] H. Brückner, T. Degenkolb, *Chem. Biodiversity* **2020**, *17*, e2000276.
- [21] J. Kleinehr, M. Schöfbänker, K. Daniel, F. Günl, F. F. Mohamed, J. Janowski, L. Brunotte, Y. Boergeling, M. Liebmann, M. Behrens, A. Gerdemann, L. Klotz, M. Esselen, H.-U. Humpf, S. Ludwig, E. R. Hrinčius, *PLoS Pathog.* **2023**, *19*, e1010986.
- [22] S. Gupta, S. B. Krasnoff, D. W. Roberts, J. A. A. Renwick, L. S. Brinen, J. Clardy, *J. Org. Chem.* **1992**, *57*, 2306.
- [23] A. Jegorov, V. Mattha, T. Trnka, M. Černý, *J. High Resolut. Chromatogr.* **1990**, *13*, 718.
- [24] S. B. Krasnoff, S. Gupta, R. J. S. Leger, J. A. A. Renwick, D. W. Roberts, *J. Invertebr. Pathol.* **1991**, *58*, 180.
- [25] M. Muroi, N. Shiragami, A. Takatsuki, *Biochem. Biophys. Res. Commun.* **1994**, *205*, 1358.
- [26] S. Matic, D. A. Geisler, I. M. Møller, S. Widell, A. G. Rasmusson, *Biochem. J.* **2005**, *389*, 695.
- [27] W. G. Bessler, B. Ottenbreit, G. Irmscher, G. Jung, *Biochem. Biophys. Res. Commun.* **1979**, *87*, 99.
- [28] E.-J. Song, E. España, S.-M. Shim, J.-H. Nam, J. Kim, K. Lee, S.-K. Park, C.-K. Lee, J.-K. Kim, *Sci. Rep.* **2021**, *11*, 9427.
- [29] A. Iida, M. Sanekata, T. Fujita, H. Tanaka, A. Enoki, G. Fuse, M. Kanai, P. J. Rudewicz, E. Tachikawa, *Chem. Pharm. Bull.* **1994**, *42*, 1070.
- [30] C. M. Boot, T. Amagata, K. Tenney, J. E. Compton, H. Pietraszkiewicz, F. A. Valeriote, P. Crews, *Tetrahedron* **2007**, *63*, 9903.
- [31] A. P. Desbois, P. J. Coote, *Adv. Appl. Microbiol.* **2012**, *78*, 25.
- [32] A. R. Bandani, B. P. S. Khambay, J. L. Faull, R. Newton, M. Deadman, T. M. Butt, *Mycol. Res.* **2000**, *104*, 537.
- [33] A. R. Bandani, B. Amiri, T. M. Butt, R. Gordon-Weeks, *Biochim. Biophys. Acta Biomemb.* **2001**, *1510*, 367.
- [34] H. C. Chen, C. K. Chou, C. M. Sun, S. Farn Yeh, *Antiviral Res.* **1997**, *34*, 137.
- [35] C. Dong, J. Yu, Y. Zhu, C. Dong, *Indian J. Med. Res.* **2013**, *138*, 969.
- [36] N. Arakaki, T. Nagao, R. Niki, A. Toyofuku, H. Tanaka, Y. Kuramoto, Y. Emoto, H. Shibata, K. Magota, T. Higuti, *Mol. Cancer Res.* **2003**, *1*, 931.
- [37] H. A. Lardy, D. Johnson, W. C. McMurray, *Arch. Biochem. Biophys.* **1958**, *78*, 587.

- [38] G. Mahmoudabadi, R. Milo, R. Phillips, *Proc. Natl. Acad. Sci. U.S.A.* **2017**, *114*, E4324–E4333.
- [39] L. Ren, W. Zhang, J. Zhang, J. Zhang, H. Zhang, Y. Zhu, X. Meng, Z. Yi, R. Wang, *Virologica Sinica* **2021**, *36*, 1532.
- [40] J. B. Ritter, A. S. Wahl, S. Freund, Y. Genzel, U. Reichl, *BMC Syst. Biol.* **2010**, *4*, 61.
- [41] S. L. Chi, S. V. Pizzo, *Ann. Med.* **2006**, *38*, 429.
- [42] T. Gorai, H. Goto, T. Noda, T. Watanabe, H. Kozuka-Hata, M. Oyama, R. Takano, G. Neumann, S. Watanabe, Y. Kawaoka, *Proc. Natl. Acad. Sci. U.S.A.* **2012**, *109*, 4615.
- [43] E. K. W. Hui, D. P. Nayak, *Virology* **2001**, *290*, 329.

SUPPORTING INFORMATION

Additional supporting information can be found online in the Supporting Information section at the end of this article.

How to cite this article: J. Eichberg, M. Oberpaul, C. Hartwig, A. H. Geißler, C. Culmsee, A. Vilcinskas, E. Böttcher-Friebertshäuser, H. Brückner, T. Degenkolb, K. Hardes, *Arch. Pharm.* **2024**;357:e2400384. <https://doi.org/10.1002/ardp.202400384>